2012

Chemically isolating hot spots on concave nanocubes

Rycenga, Matthew

American Chemical Society

M. Rycenga, M.R. Lagillel, M.L. Personick, T. Ozel, C.A. Mirkin, "Chemically isolating hot spots on concave nanocubes," Nano Letters, v.12, (2012), pp. 6218-6222.
http://hdl.handle.net/10945/52427

NANO LETTERS

Letter

pubs.acs.org/NanoLett

Chemically Isolating Hot Spots on Concave Nanocubes

Matthew Rycenga, Mark R. Langille, Michelle L. Personick, Tuncay Ozel, and Chad A. Mirkin*

Department of Chemistry and International Institute of Nanotechnology, Northwestern University, Evanston, Illinois 60208, United States

Supporting Information

ABSTRACT: We report a simple and general strategy for selectively exposing and functionalizing the sharp corners of concave nanocubes, which are the SERS hot spots for such structures. This strategy takes advantage of the unique shape of the concave cubes by coating the particles with silica and then etching it away to expose only the corner regions, while maintaining the silica coating in the concave faces. These corner regions can then be selectively modified for improved enhancement and signal response with SERS.

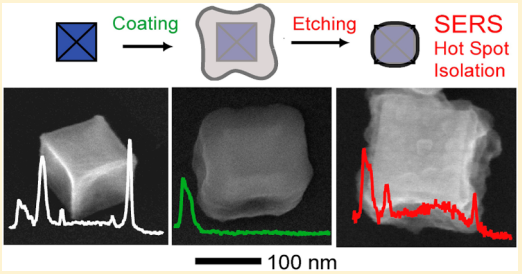

KEYWORDS: *Anisotropic nanoparticle, hot spot, surface-enhanced Raman scattering, concave nanocube*

Nanoparticle shape is a structural parameter that allows researchers to control optical, magnetic, electrical, and catalytic properties.[1−6] Such control is extremely important with respect to noble metal nanoparticles, where shape and size dictate the plasmonic properties of structures. Consequently, many synthetic strategies have been developed to synthesize noble metal nanoparticles of a wide variety of sizes and shapes.[2,7−13] Examples realized thus far include cubes,[11] tetrahedra,[14] octahedra,[15] rods,[3,16] bipyramids,[17] bars,[18] wires,[19] polygonal plates,[4,8] and many others.[20] As researchers gain greater control over particle shape, new opportunities and challenges arise for face, corner, and edge-selective functionalization.[21] For example, rods can be selectively functionalized on their opposing ends,[22] triangular prisms on their edges and faces,[23] and cubes on specific faces.[24] Techniques developed thus far take advantage of either the inherent differences in reactivity of different faces or the ability to arrange and mask certain parts of anisotropic particles so that selective functionalization is possible. These methods for face and edge-selective functionalization are becoming extremely important in the area of programmable self-assembly where they allow one to introduce the concept of valency.[25−28]

Certain particle synthesis methods provide routes to unusual structures with high-index facets, like the {720}-faceted Au concave nanocubes.[29] These structures have a cube shape with well-defined sharp corners but with square pyramid-shaped depressions in each one of the six faces (Figure 1A,B). This type of structure provides additional opportunities for selective functionalization, and herein, we show how they can be used to uniquely create structures with corners that are selectively exposed and modifiable. Moreover, we demonstrate how they can be utilized to prepare particles with uniform and high enhancement factors in the context of surface-enhanced Raman spectroscopy (SERS) studies.

The ability to synthesize unusual nanoparticle structures with tight control over architectural parameters has led to advances in SERS; in particular, certain structures have "hot spots" that exhibit large enhancement factors (EFs).[30,31] These hot spots typically represent a small fraction of the total surface area, and their formation is dependent on many factors, especially nanoparticle shape.[32−34] This is clearly evident if one compares the SERS from individual concave nanocubes, nanocubes, and spherical nanoparticles functionalized with a monolayer of 1,4-benzenedithiol (1,4-BDT), Figure 1. The vibrational signal for the 8A band of 1,4-BDT at 1565 cm^{-1} can be used to estimate the EF of each structure under optimum conditions. For example, the 1565 cm^{-1} band is ∼60 times greater on the concave cube as compared with the normal cube and is not observed on the spheres when excited at 785 nm, a wavelength that is optimum for the concave cube as it is in resonance with its LSPR (Figure 1I, blue trace). Note that, to optimize the SERS on each of these structures, we studied a variety of different sized concave nanocubes (114 ± 9 nm and 50 ± 20 nm), nanocubes (108 ± 15 nm and 150 ± 20 nm), and spherical nanoparticles (115 ± 6 nm and 140 ± 11 nm) and evaluated their responses at two excitation wavelengths (633 and 785 nm). The highest EFs at optimized excitation wavelengths were $1.4 \times 10^6 \pm 0.1 \times 10^6$ for the concave nanocubes (edge length 114 ± 9 nm), $4.8 \times 10^4 \pm 8 \times 10^3$ for the nanocubes (edge length 108 ± 15 nm), and $6.1 \times 10^3 \pm 0.7 \times 10^3$ for the spherical particles (diameter 115 ± 6 nm). Note that 633 nm is more optimum for the spheres and the nanocubes as it is in resonance with their LSPRs (Figure 1I, black and red traces, respectively). These EF calculations were based upon a minimum of 30 measurements on each particle

Received: August 29, 2012
Revised: October 25, 2012
Published: November 8, 2012

dx.doi.org/10.1021/nl3032235 | *Nano Lett.* 2012, 12, 6218−6222

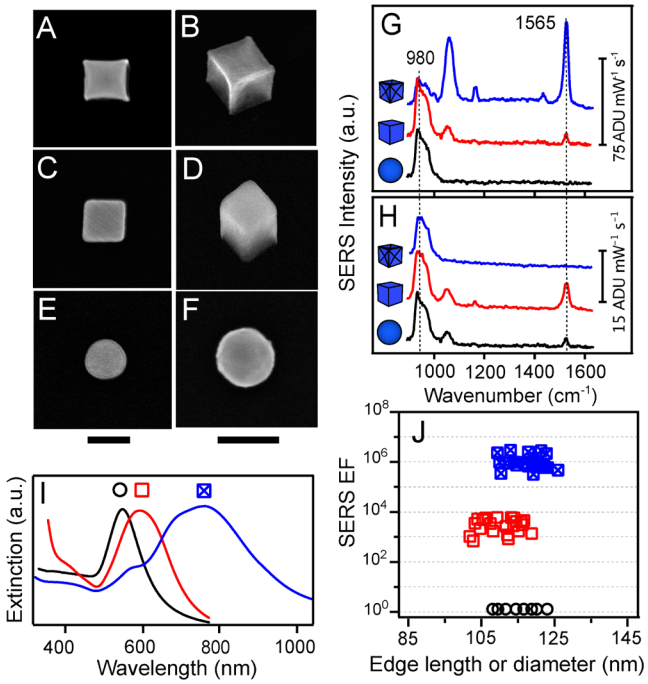

Figure 1. (A-F) Typical single-particle scanning electron microscope (SEM) images of Au concave nanocubes (A, B), nanocubes (C, D), and spherical nanoparticles (E, F) at 0° and 45°, respectively. Each scale bar is 100 nm. (G, H) The corresponding SERS from the individual nanoparticles at two excitation wavelengths, 785 nm (G) and 633 nm (H), functionalized with the molecule 1,4-BDT (band at 1565 cm^{-1}) and deposited on a Si substrate (band at ~980 cm^{-1}). In each plot, the top spectrum is from a concave nanocube (blue trace), the middle from a nanocube (red trace), and the bottom from a spherical nanoparticle (black trace). (I) The extinction spectra of the nanoparticles used in (G, H) suspended in water. Concave cubes are indicated by crossed blue squares, cubes as red squares, and spheres as black circles. (J) A plot of the EFs from the single nanoparticles in this study excited with a 785 nm laser as a function of the length of their edge or diameter.

type where the laser polarization was along the diagonal of the concave nanocube or nanocube. The standard deviation of the EFs for the concave cubes was ~7% and is a testament to the high degree of uniformity of the samples. The standard deviations of the EFs for nanocubes and spheres were ~16% and ~11%, respectively.

The trends in the SERS data shown in Figure 1 can be understood in the context of the surface curvature of the nanoparticles because regions of large surface curvature typically exhibit larger near-field enhancements or hot spots.[35] From zoomed-in tranmission electron microscope (TEM) images of a corner region from each of the nanoparticles (Figure 2), we determined the radius of curvature (see red dashed line) of the corners of a concave cube to be approximately 2 nm. In contrast the nanocubes have a larger corner curvature (19 nm), and the spheres have a very large surface curvature (100 nm). Indeed, these concave cubes exhibit extremely sharp corners and, therefore, have the prospect for the formation of highly localized hot spots and large electromagnetic-field enhancements. Consistent with this hypothesis, finite-difference time-domain (FDTD) near-field simulations for each nanoparticle shape show a near-field enhancement (E^2) of 150, 25, and 20 at 1 nm from the corners of the concave cubes and normal cubes and the surface of a sphere, respectively (Figure 2A–C). Taken together, the data in Figures 1 and 2 illustrate how shape control of metal nanoparticles can be used to deliberately tailor and optimize the SERS behavior of noble metal nanostructures, and more specifically, that the SERS signal from concave cubes will likely derive primarily from their sharp corners.

However, in principle, even metal nanoparticles with the same morphology and excited under the same excitation parameters can generate different SERS signal intensities and EFs based upon the extent of the molecular coverage on the nanoparticle. When a nanoparticle is completely functionalized, signal reproducibility (from nanostructure-to-nanostructure) is dependent on the excitation parameters and the monodispersity of the particle's morphology throughout the sample. When there is incomplete surface functionalization, this is no longer the case. This is clearly evident when one probes the SERS signals from concave cubes (and hence EFs) as a function of surface coverage with 1,4-BDT (Figure 2G). At short functionalization times (which leads to incomplete coverage), the standard deviation of the SERS signal from the concave cubes approaches ~30%. At longer modification times the intensity distribution attenuates, until the distribution reaches approximately 8%. Note the morphology of the particle, as measured by TEM and SEM, remains unchanged under these conditions. The fact that signal reproducibility is poor in the low-molecule coverage regimes (regardless of the high degree

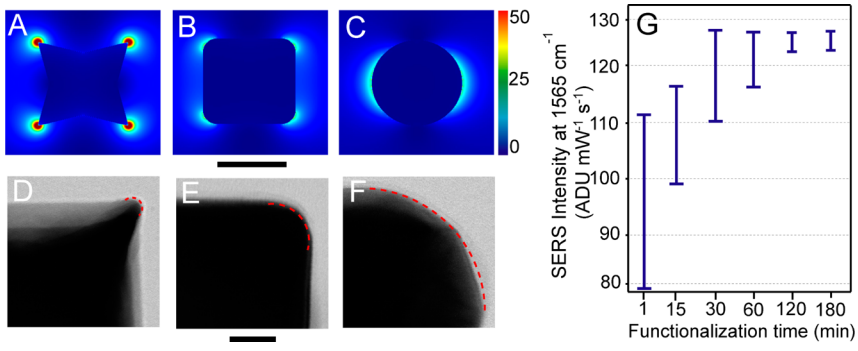

Figure 2. (A–C) FDTD simulations of the near-field enhancements (E^2) plotted for a concave nanocube (A), nanocube (B), and a nanosphere (C), in air with 785 nm excitation. The scale bar is 100 nm. (D–F) TEM images of a corner region on a concave nanocube (D), nanocube (E), and spherical nanoparticle (F). The scale bar is 30 nm. The red dashed line was used to calculate the radius of curvature of the particles. (G) A plot of the SERS signal intensity from the molecule 1,4-BDT (band at 1565 cm^{-1}) from single concave cubes as a function of the functionalization time with 1,4-BDT.

dx.doi.org/10.1021/nl3032235 | *Nano Lett.* 2012, 12, 6218–6222

of sample uniformity) is a significant problem for SERS, since this is the regime wherein SERS could be most useful as a sensing modality.

In this Letter, we aimed to take advantage of the unique morphology of the concave cubes to expose only the corner regions to exogenous molecules, effectively isolating the hot spot regions. We hypothesized that this would eliminate unwanted signal fluctuation at low molecular coverage because the molecules could only adsorb in regions with similar near-field enhancements. To isolate the corner regions of the concave cubes, the particles were coated with SiO_2 using a modified Stöber process,[36] and then the SiO_2 was carefully etched away with NaOH (Figure 3A). Although the Au

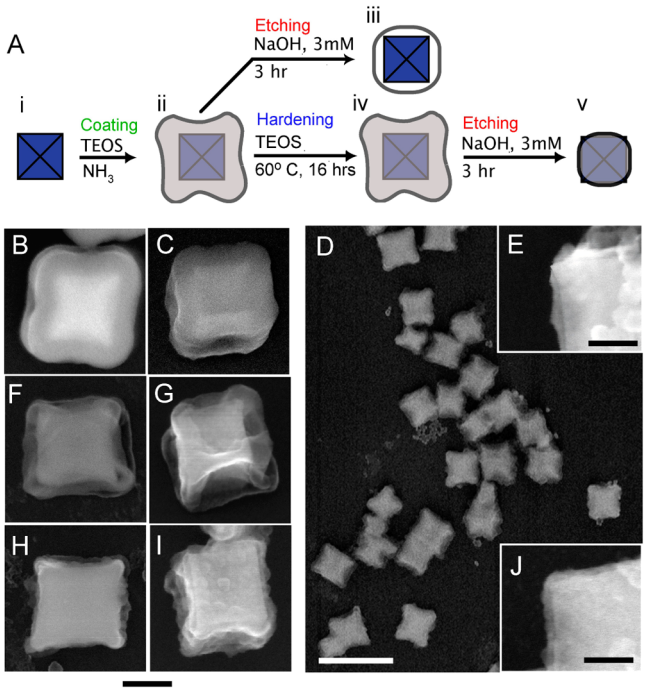

Figure 3. (A) Procedure used to coat concave cubes with SiO_2 shells using TEOS and NH_3, harden the shells, and etch the shells with NaOH to expose the corners of the concave cube. (B, C) SEM images of SiO_2-coated concave cubes, labeled ii in A, at 0° and 45°, respectively. (F, G) SEM images of the etched SiO_2-coated concave cubes without hardening the shells, labeled iii in A. The shells are transparent and hollow. (H, I) SEM images of the etched SiO_2-coated concave cubes with hardened shells at 0° and 45°, labeled v in A. Scale bar is 50 nm. (D) Typical SEM image of the product formed from etching the hardened shells. Scale bar is 200 nm. (E) SEM of a concave cube with a hardened shell that shows a corner exposed and (J) the corner not exposed. Both were present in the final product (D). Scale bars are 30 nm.

particles were capped with cetyltrimethyammounium chloride (CTAC), we found no difficulty in coating the concave cubes with a SiO_2 shell at several thicknesses ranging from 10 to 60 nm. The shell thickness could be controlled by the reaction time and the concentration of tetraethylorthosilicate (TEOS) (Supporting Information for experimental; Figure 3B,C).

Our initial attempts at etching the silica shell with NaOH resulted in hollowed-out shells, with the outer part of the shell intact, and the inner portion of the silica shell near the Au particle removed (Figure 2F,G). At longer etch times, the shell hollows out completely and, eventually, collapses (Figure S4 of the SI). The key to uniform etching of the silica shell is to ensure that the shell has a uniform chemical composition, as observed recently by others.[37] The nature of the shell on the concave cubes is critical. We targeted shells that had a high degree of cross-linking and that would likely exhibit uniform outside-in etching behavior as opposed to nonuniform behavior known to produce hollow structures.[37] Optimum shells were synthesized by slow growth of the shell (i.e., growth over a period of 18 h) and alternatively by introducing a hardening step that consisted of heating the as-prepared silica-coated concave cube sample in anhydrous ethanol for 16 h with a trace amount of TEOS. Consistent with the formation of a hardened shell, the shells etch from the outside-in, and the Au concave cube cores take much longer (6−8 h longer under identical conditions) to dissolve in KCN (Figure S5). With the hardened samples, a strong base was used to successfully etch away the silica shells uniformly. With 3 mM NaOH, the etch rate was approximately 5−10 nm per hour for the silica-coated concave cubes. Using this estimation, we prepared samples of silica-coated concave cubes with only the Au corner regions exposed at yields of ∼50% (Figure 3D,E). Note that the same coating/etching procedure with nanocubes did not result in corner-isolated regions (Figure S6).

TEM imaging was used to determine that 5 ± 4 nm of the Au tip (measured along the edge) of the concave cube was protruding from the SiO_2 shell. During functionalization of these structures, 1,4-BDT will bind exclusively to the exposed Au corner regions as it has no appreciable affinity for SiO_2. Even with nonspecific adsorption of 1,4-BDT to the silica shell, the molecules will be physically away from the surface of the Au concave cube, where the near-fields are highly localized and decay exponentially from the Au surface.[35,38] The SERS responses for four differently prepared silica-coated concave cubes were studied to determine the effects of isolating the corner regions for selective functionalization (Figure 4). For silica-coated concave cube samples with no exposed Au regions (Figure 4A, B), there is no SERS signal from the 1,4-BDT, regardless of the hardness of the shell (compare Figures 4A, B, and E, blue and red traces). For the concave cube that was coated with silica, which was then all subsequently etched away (Figure 4C), the SERS signal was typical of a SiO_2-free concave cube (compare Figure 4E, black trace, to Figure 1). For the concave cube with only the corner regions exposed, a SERS signal from 1,4-BDT is observed (Figure 4D and E, green trace). This signal intensity is reduced compared to a bare concave cube (Figure 4E, compare black and green traces); however if the corner regions are functionalized with 1,4-BDT (∼160 molecules per corner; recall only 5 nm is exposed), then the EF is on the order of $\sim 10^8$, 2 orders of magnitude greater than fully functionalized concave cubes. FDTD simulations of silica-coated and silica-free concave cubes do not show appreciable differences near-field enhancement (Figure S9, SI).

The SERS responses from 35 of these corner-isolated concave cubes were measured after functionalizing them with 1,4-BDT for only 1 min. The variation of the signal intensity from these structures was dramatically reduced compared to similarly functionalized (1 min) SiO_2-free concave cubes (Figure 4F). Note that, for the corner-isolated structures, there is a bimodal distribution of responses, where particles either exhibit no significant signal or a large one (green bars in Figure 4F). In contrast, the concave cubes without silica exhibit a wide variety of signal intensities (blue bars in Figure 4F). This observation is likely due to the highly delocalized functionalization of the SiO_2-free cubes as compared to the tip-localized

dx.doi.org/10.1021/nl3032235 | Nano Lett. 2012, 12, 6218−6222

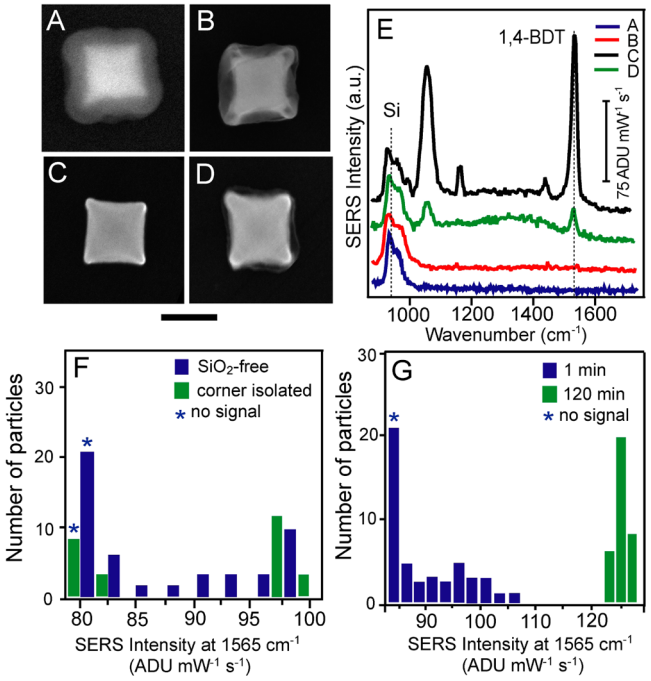

Figure 4. SEM images of concave cubes that were: (A) coated with SiO_2; (B) coated with SiO_2 and etched yielding a hollow shell; (C) coated in a SiO_2 shell, which was then completely etched away to expose the bare concave cube; and (D) coated with SiO_2, hardened, and then etched to expose the corner regions. The scale bar is 100 nm. Their corresponding single-particle SERS spectra are shown in E. No SERS signals were detected for concave cubes coated with SiO_2 (blue) or that had a hollow SiO_2 shell (red). The bare concave cubes (black) had signals that were comparable to normal SiO_2-free concave cubes. SiO_2-coated concave cubes with their corners exposed exhibited signal from 1,4-BDT (green). (F) The SERS intensity distribution (measured from the 1565 cm^{-1} band of 1,4-BDT) from single concave cubes that were SiO_2-free (blue) and corner isolated concave cubes (green). Both were functionalized with 1,4-BDT for 1 min. (G) The SERS intensity distribution measured from single, SiO_2-free, concave cubes at two different functionalization times with the molecule 1,4-BDT: 1 min (blue) and 120 min (green).

functionalization of the corner-isolated structures. This conclusion is reinforced when one studies the response of SiO_2-free cubes as a function of adsorbate coverage or functionalization time. For example, the response of SiO_2-free concave cubes at two functionalization time points, 1 and 120 min (Figure 4G), show markedly different effects. At long functionalization times, the SERS signals are tightly bundled around one set of intensities (green bars in Figure 4G), while at short functionalization times this is not the case, and the signal varies significantly (blue bars in Figure 4G). Indeed, for the SiO_2-free concave cubes at early functionalization time points, the adsorbate molecules are randomly distributed on the faces and highly enhancing tips, hence a nonuniform signal. However, at longer time points, the structures are uniformly coated with adsorbate and, therefore, give a more reproducible response. Taken together, these data suggest that corner-isolation can lead to structures with both large enhancement factors and more reproducible responses.

In conclusion, we have demonstrated a general strategy for selectively exposing and functionalizing the sharp corners of concave nanocubes, which are the SERS hot spot regions for such structures. This strategy is useful for multiple reasons. First, it can lead to larger and more consistent enhancement capabilities for such single particle nanostructures. Indeed, if single particle structures are to be used as detection labels, as opposed to the more generally used dimers,[30] strategies like the one employed herein will be necessary for increasing enhancement factors and consistency of SERS-response. Second, the method, in principle, can be generalized to other types of anisotropic nanostructures, including beveled prisms, trisoctahedra, and concave octahedra.[39] Third, the method could become quite useful for researchers, who are trying to control the spatial distribution of molecules on a nanoparticle's surface in efforts to create nanoparticle valency.[25] Such valency control is especially important in the area of programmable colloidal assembly based upon peptide- and nucleic-acid-nanoparticle conjugates.[26−28]

■ ASSOCIATED CONTENT

Supporting Information

Experimental details, SERS characterization of the nanostructures, and images of the silica coated concave cubes at various stages of coating and etching. This material is available free of charge via the Internet at http://pubs.acs.org.

■ AUTHOR INFORMATION

Corresponding Author

*E-mail: chadnano@northwestern.edu.

Notes

The authors declare no competing financial interest.

■ ACKNOWLEDGMENTS

This material is based upon work supported by the DoD/NSSEFF Program/Naval Postgraduate School under Award No. N00244-09-1-0012 and Award No. N00244-09-1-0071. Any opinions, findings, and conclusions or recommendations expressed in this publication are those of the authors and do not necessarily reflect the views of the DoD/NSSEFF Program/NPS. This material is also based upon work supported by the AFOSR under Award No. FA9550-09-1-0294, the National Science Foundation's MRSEC program (DMR-0520513 and DMR-1121262) at the Materials Research Center of Northwestern University, and the Non-equilibrium Energy Research Center (NERC), an Energy Frontier Research Center funded by the U.S. Department of Energy, Office of Science, Office of Basic Energy Sciences under Award Number DE-SC0000989.

■ REFERENCES

(1) Millstone, J. E.; Park, S.; Shuford, K. L.; Qin, L.; Schatz, G. C.; Mirkin, C. A. *J. Am. Chem. Soc.* **2005**, *127*, 5312.
(2) Jin, R.; Cao, Y.; Mirkin, C. A.; Kelly, K. L.; Schatz, G. C.; Zheng, J. G. *Science* **2001**, *294*, 1901.
(3) Hurst, S. J.; Payne, E. K.; Qin, L.; Mirkin, C. A. *Angew. Chem., Int. Ed.* **2006**, *45*, 2672.
(4) Millstone, J. E.; Hurst, S. J.; Metraux, G. S.; Cutler, J. I.; Mirkin, C. A. *Small* **2009**, *5*, 646.
(5) Xia, Y.; Xiong, Y.; Lim, B.; Skrabalak, S. E. *Angew. Chem., Int. Ed.* **2009**, *48*, 60.
(6) Tao, A. R.; Habas, S.; Yang, P. *Small* **2008**, *4*, 310.
(7) Maillard, M.; Huang, P.; Brus, L. *Nano Lett.* **2003**, *3*, 1611.
(8) Jin, R.; Charles Cao, Y.; Hao, E.; Metraux, G. S.; Schatz, G. C.; Mirkin, C. A. *Nature* **2003**, *425*, 487.
(9) Zhang, J.; Li, S.; Wu, J.; Schatz, G. C.; Mirkin, C. A. *Angew. Chem., Int. Ed.* **2009**, *48*, 7787.

(10) Xue, C.; Millstone, J. E.; Li, S.; Mikin, C. A. *Angew. Chem., Int. Ed* **2007**, *46*, 8436.
(11) Sun, Y.; Xia, Y. *Science* **2002**, *298*, 2176.
(12) Kim, F.; Connor, S.; Song, H.; Kuykendall, T.; Yang, P. *Angew. Chem., Int. Ed.* **2004**, *43*, 3673.
(13) Wang, C.; Daimon, H.; Onodera, T.; Koda, T.; Sun, S. *Angew. Chem., Int. Ed.* **2008**, *47*, 3588.
(14) Wiley, B. J.; Herricks, T.; Sun, Y.; Xia, Y. *Nano Lett.* **2004**, *4*, 1733.
(15) Langille, M. R.; Personick, M. L.; Zhang, J.; Mirkin, C. A. *J. Am. Chem. Soc.* **2011**, *133*, 10414.
(16) Zhang, J.; Langille, M. R.; Mirkin, C. A. *Nano Lett.* **2011**, *11*, 2495.
(17) Personick, M. L.; Langille, M. R.; Zhang, J.; Harris, N.; Schatz, G. C.; Mirkin, C. A. *J. Am. Chem. Soc.* **2011**, *133*, 6170.
(18) Wiley, B. J.; Wang, Z. L.; Wei, J.; Yin, Y.; Cobden, D. H.; Xia, Y. *Nano Lett.* **2006**, *6*, 2273.
(19) Sun, Y.; Gates, B.; Mayers, B. T.; Xia, Y. *Nano Lett.* **2006**, *2*, 165.
(20) Glotzer, S. C. *Science* **2004**, *306*, 419.
(21) Glotzer, S. C.; Solomon, M. J. *Nat. Mater.* **2007**, *6*, 557.
(22) Nie, Z.; Fava, D.; Kumacheva, E.; Zou, S.; Walker, G. C.; Rubinstein, M. *Nat. Mater.* **2007**, *6*, 609.
(23) Millstone, J.; Georganopoulou, D.; Xu, X.; Wei, W.; Li, S.; Mirkin, C. *Small* **2008**, *4*, 2176.
(24) Rycenga, M.; McLellan, J. M.; Xia, Y. *Adv. Mater.* **2008**, *20*, 2416.
(25) Jones, M. R.; Macfarlane, R. J.; Lee, B.; Zhang, J.; Young, K. L.; Senesi, A. J.; Mirkin, C. A. *Nat. Mater.* **2010**, *9*, 913.
(26) Macfarlane, R.; Jones, M.; Senesi, A.; Young, K.; Lee, B.; Wu, J.; Mirkin, C. *Angew. Chem., Int. Ed.* **2010**, *49*, 4589.
(27) Xu, X.; Rosi, N. L.; Wang, Y.; Huo, F.; Mirkin, C. *J. Am. Chem. Soc.* **2006**, *128*, 9286.
(28) Li, M.; Schnablegger, H.; Mann, S. *Nature* **1999**, *402*, 393.
(29) Zhang, J.; Langille, M. R.; Personick, M. L.; Zhang, K.; Li, S.; Mirkin, C. A. *J. Am. Chem. Soc.* **2010**, *132*, 14012.
(30) Banholzer, M. J.; Millstone, J. E.; Qin, L.; Mirkin, C. A. *Chem. Soc. Rev.* **2008**, *37*, 885.
(31) Li, W.; Camargo, P. H. C.; Au, L.; Zhang, Q.; Rycenga, M.; Xia, Y. *Angew. Chem., Int. Ed.* **2010**, *49*, 164.
(32) Qin, L.; Zou, S.; Xue, C.; Atkinson, A.; Schatz, G. C.; Mirkin, C. A. *Proc. Natl. Acad. Sci.* **2006**, *103*, 13300.
(33) Qin, L.; Banholzer, M.; Millstone, J.; Mirkin, C. *Nano Lett.* **2007**, *7*, 3849.
(34) Cao, Y. C.; Jin, R.; Nam, J. M.; Thaxton, C. S.; Mirkin, C. A. *J. Am. Chem. Soc.* **2003**, *125*, 14677.
(35) Kelly, K.; Coronado, E.; Zhao, L.; Schatz, G. *J. Phys. Chem. B* **2003**, *107*, 668.
(36) Stöber, W.; Fink, A.; Bohn, E. *J. Colloid Interface Sci.* **1968**, *62*, 26.
(37) Wong, Y. J.; Zhu, L.; Teo, W. S.; Tan, Y. W.; Yang, Y.; Wang, C.; Chen, H. *J. Am. Chem. Soc.* **2011**, *133*, 11422.
(38) Ru, E. C. L.; Etchegoin, P. G.; Meyer, M. *J. Chem. Phys.* **2006**, *125*, 204701.
(39) Xia, X.; Zeng, J.; McDearmon, B.; Zheng, Y.; Li, Q.; Xia, Y. *Angew. Chem., Int. Ed.* **2011**, *50*, 12542.